NMR of Silk Fibroin. 2. ^{13}C NMR Study of the Chain Dynamics and Solution Structure of *Bombyx mori* Silk Fibroin

Tetsuo Asakura,* Yasuo Watanabe, Akane Uchida, and Hidenobu Minagawa

Department of Biopolymer Engineering, Faculty of Technology, Tokyo University of Agriculture and Technology, Koganei, Tokyo 184, Japan. *Received March 24, 1983*

ABSTRACT: ^{13}C NMR spectroscopy has been applied to the chain dynamics of *B. mori* silk fibroin in solution and the silk fibroin stored in the silk gland of the intact silkworm. All the peaks were sharp except for the C^{α} and C=O peaks of the Gly residue and the C=O peak of the Ala residue: a slight splitting was observed for these latter peaks, indicating sensitivity to the amino acid sequence of the silk fibroin. The amino acid composition determined by ^{13}C NMR spectroscopy was very close to that for silk fibroin determined from amino acid analysis, indicating that both domains, i.e., crystalline and noncrystalline, in the fibrous protein were observed in the spectrum. The mean correlation times of the segmental motion, determined from the spin–lattice relaxation times and nuclear Overhauser enhancements of the Ala, Gly, and Ser C^{α} carbons assuming a log χ^2 distribution model, were of the order of 10^{-10} s at 40 °C. Moreover, the width parameter, p, in the model was determined to be 11–14, indicating a broad distribution of correlation times. These are typical of a random coil polymer. The rate of internal rotation around the C^{α}–C^{β} bond decreases in the order Ala, Ser, Tyr. The side-chain motion is strongly hindered for the Tyr residue although the pK_a value for Tyr OH deprotonation indicates absence of intra- or intermolecular hydrogen bonding between the OH group and any amino acid residues of the silk fibroin. A decrease in the T_1 values and an increase of the mean correlation times of the segmental motion were observed with increasing concentration. This is discussed in relation to the appearance of the silk I type conformation accompanying the aggregation of the chain.

Introduction

NMR spectroscopy has proved quite useful in studying the dynamics and structural properties of some fibrous proteins such as elastin or collagen in both solution and solid states.[1] However, the NMR method has received only limited application to silk fibroin. We have recently shown that ^{13}C NMR spectroscopy is useful in characterizing the conformation of the silk fibroin stored in the silk gland of intact silkworms by monitoring the conformation-dependent peak behavior of the Ala residue.[2] Saito et al.[3] and Kricheldorf et al.[4] applied solid-state high-resolution ^{13}C NMR (CP/MAS NMR) to the conformational characterization of silk fibroins in the solid state.

In the present paper, ^{13}C NMR spectroscopy is applied to the chain dynamics of the silk fibroin of *B. mori* in solution and also of the silk fibroin stored in the middle silk gland of the intact mature larva.[5] The ^{13}C nucleus is particularly suited for dynamics studies because the interpretation of the relaxation parameters, i.e., spin–lattice relaxation time, T_1, and nuclear Overhauser enhancement, NOE, are generally not complicated by intermolecular relaxation processes, unlike the situation for ^1H and ^{19}F nuclei. Particularly for protonated ^{13}C nuclei, the relaxation is generally dominated by a single mechanism: the intramolecular ^{13}C–^1H dipolar interaction with directly bonded protons.[6] Moreover, the large chemical shift range of the ^{13}C nucleus makes it possible to resolve most individual carbons, and thus multiple sites are often available at which to probe a molecule's motional features. Silk fibroin, a nonglobular protein, is expected to exhibit dynamic characteristics similar to those of polymers where the molecular-weight-independent segmental motion of the chain can contribute significantly to the T_1 and NOE values.[7] Such segmental motion of a long chain seems to be characterized by a distribution of correlation times because the correlation times associated with the many possible cooperative interactions between monomer units in the chain may be occurring on different time scales. We use a log χ^2 distribution model[8] in the interpretation of the relaxation data for silk fibroin. This model has been successfully used in chain dynamics studies of synthetic polymers such as poly(methyl methacrylate),[9–11] polystyrene,[8,10] polypropylene,[12] and poly(but-1-ene)[12] and polypeptides such as poly(L-lysine), poly(L-arginine), and poly(L-ornithine)[13] as well as elastin,[1] a fibrous protein.

In addition, the pH dependence of the chemical shifts are observed at different concentrations of the *B. mori* silk fibroin and are compared with those observed for *N*-acetyl amino acid methylamides, Ac-X-NHMe, where X = Gly, L-Ala, L-Ser, L-Tyr, and L-Val. In particular, we can judge from the pK_a value of the deprotonation of the Tyr OH group in silk fibroin whether a hydrogen bond is formed between any amino acid residue and the OH group.[14]

Experimental Section

Materials. Raw silk or the cocoon of *B. mori* was degummed twice with 0.5% Marseilles soap solution at 100 °C for 0.5 h and then washed with distilled water. Then the silk was dissolved in 9 M LiBr at 40 °C. After dialysis against distilled water for 4 days, the solution was clarified by spinning in a centrifuge at 10 000 rpm for 20–30 min. The supernatant was collected and brought gently up to the desired concentration with an electric fan.

A silkworm of *B. mori*, a hybrid between strains Nichi 140 and Shi 140, was used for direct ^{13}C NMR determination of T_1.[15]

Ac-L-Ala-NHMe was synthesized from L-alanine as described previously.[16] Ac-X-NHMe, where X = Gly and L-Ser, were synthesized from the corresponding amino acid hydrochloride according to the method of Applewhite and Niemann[17] and Ac-X-NHMe, where X = L-Tyr and L-Val, were derived from the corresponding ester compounds. All starting materials were purchased from Kokusan Chemical Ltd.

Method. Proton-noise-decoupled ^{13}C NMR spectra were observed at 40 °C with a JEOL FX-200 NMR spectrometer operating at 50 MHz equipped with a temperature controller. The spectral width was 12 000 Hz with 16K data points. The spin–lattice relaxation times, T_1, measured only for the protonated carbons, were made by the inversion–recovery method, i.e., by 180°–τ–90° pulse sequences, using between 8 and 11 τ values. The T_1 values were determined by using the peak areas, which were measured by cutting out and weighing traces of the peaks. The NOE values were determined by direct comparison of peak areas obtained with complete ^1H decoupling to the corresponding areas obtained with the gated ^1H decoupling method. The ratio of the pulse delay to T_1 was 10 for the gating experiments to avoid the problems noted by Opella et al.[18] The sample concentration was varied from 2.1% to 14.5% and a small amount of ^2H_2O (5%) was added to the aqueous solution. In the intact NMR observation,[15] the middle silk gland with the part of the silkworm containing it was exposed to the magnetic field over a length of $\simeq$1 cm. Sample spinning and magnetic field locking with a ^2H signal were not used. The ^1H nuclei were decoupled only during

0024-9297/84/2217-1075$01.50/0

Table I
^{13}C NMR Chemical Shifts in *B. mori* Silk Fibroin, Ac-X-NHMe, and *P. c. ricini* Silk Fibroin[a]

amino acid	in aqueous solution	in *B. mori* mature larva	in 8 M urea solution	Ac-X-NHMe[d]	in *P. c. ricini* mature larva
Gly					
C^{α}	42.7	42.6	42.6	42.6	42.7
C=O	171.3[b]	171.3[b]	171.1[b]	172.0	171.8
	171.7[c]	171.6[c]	171.5[c]		
Ala					
C^{α}	50.0	50.0	50.0	49.8	51.5 (h)[e]
					50.1 (c)
C^{β}	16.6	16.7	16.6	16.7	15.7 (h)
					16.4 (c)
C=O	175.5	175.5	175.5	175.6	177.2 (h)
					175.7 (c)
Ser					
C^{α}	55.9	55.9	55.9	55.8	55.6
C^{β}	61.3	61.3	61.4	61.2	61.4
C=O	172.4	172.5	172.4	172.2	
Tyr					
C^{α}	55.4		55.5	55.6	
C^{β}	36.1	36.4	36.2	36.4	36.2
C^{γ}	128.0	128.0	128.0	128.4	
C^{δ}	130.5	130.5	130.5	130.4	130.5
C^{ϵ}	115.5	115.4	115.6	115.4	115.6
C^{ζ}	154.6	154.6	154.7	154.5	154.8
C=O	173.7	173.7	173.7		173.8
Val					
C^{α}	59.8	59.3	59.7	59.9	
C^{β}	30.0			29.8	
$C^{\gamma 1}$	18.4		18.4	18.3	
$C^{\gamma 2}$	17.6		17.5	17.5	
Thr					
C^{α}	59.4				
C^{β}	67.4				
C^{γ}	18.9				
Phe					
C^{α}					
C^{β}					
C^{γ}	136.5				
C^{δ}	129.1				
C^{ϵ}	128.7				
C^{ζ}	127.1				
C=O					

[a] The values are represented in ppm from external $(CH_3)_4Si$. [b] For the Ala-*Gly*-Ala sequence. [c] For the Ala-*Gly*-Ser sequence. [d] X = Gly, L-Ala, L-Ser, L-Val, and L-Tyr. [e] h, helix peak; c, coil or silk I peak.

the sampling time of 0.34 s (8K data points) to avoid an increase of temperature in the sample tube. Chemical shifts were measured in ppm downfield from the external HMDS reference and corrected to the external $(CH_3)_4Si$ reference by adding 1.96 ppm. For the chemical shift determination in intact silkworms, the main methylene peak of the triglyceride was used as the reference (29.9 ppm).[15] The pH of the solution was determined with a TP-101 pH meter with a complex electrode of the combination microelectrode CE 103C of the Toko Chemical Laboratories Co., Ltd. To avoid hydrolysis of the silk fibroin, the NMR observations at pH ≥13 were performed within 0.5 h.

Results

^{13}C NMR Spectra. Figure 1 shows the ^{13}C NMR spectrum of the regenerated silk fibroin of *B. mori*. The assignment was readily performed by reference to the chemical shifts of Ac-X-NHMe (where X = Gly, L-Ala, L-Ser, L-Tyr, or L-Val) and of the small peptides reported elsewhere.[19] The Gly, L-Ala, L-Ser, L-Tyr, and L-Val residues, of which silk fibroin has relatively large amounts, give well-resolved spectra. There are small but explicit peaks which are assigned to the L-Phe and L-Thr residues. All peaks are sharp; i.e., the half-height width is 3.4 Hz as an average, except for the C^{α} and C=O peaks of the Gly residue and C=O peak of the Ala residue, indicating high mobility of the silk fibroin chain. Fine structure was observed for the Gly and Ala C=O peaks and also for the peak of the C^{α} carbon of the Gly residue. These are considered to be reflections of the amino acid sequence of the silk fibroin rather than the conformation since a significant change in the spectra is not observed on adding urea to the solution. For example, a peak at 171.7 ppm is assigned to Gly C=O in the Ala-*Gly*-Ser sequence because the peak intensity is the same as that of Ser C=O. Another peak, 171.3 ppm, in the Gly C=O resonance region is tentatively assigned to the Ala-*Gly*-Ala sequence. The detailed sequence analysis is now proceeding in our laboratory using ^{13}C- or ^{15}N-labeled silk fibroin.

The chemical shift data for the regenerated silk fibroin from *B. mori* are listed in Table I. The values of the silk fibroins in *B. mori* mature larva, 8 M urea solution, *P. c. ricini* mature larva, and Ac-X-NHMe (X = Gly, L-Ala, L-Ser, L-Tyr, or L-Val) are also summarized. The chemical shifts in all the amino acid residues of *B. mori* silk fibroin are in fair agreement among the 14.5% aqueous solution, liquid silk in mature larva, and 8 M urea solution. Moreover, the chemical shifts of the regenerated silk fibroin are essentially independent of concentration in the range 0.3–14.5%. In contrast to the spectra of *B. mori* silk fibroin, doublet peaks were observed for the Ala C^{α},[20] C^{β}, and C=O carbons in the spectrum of the silk fibroin of *P. c. ricini*. The peak positions of the low-field component of Ala C^{β} and the high-field components of Ala C^{α} and

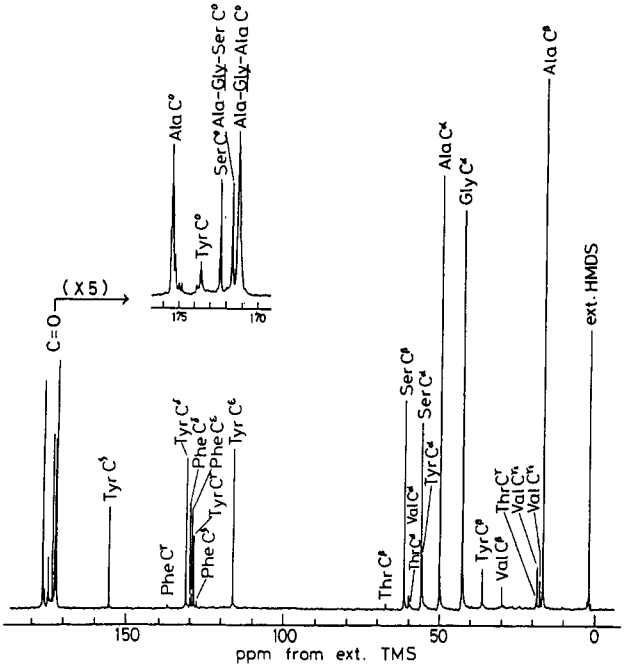

Figure 1. Proton-noise-decoupled ^{13}C NMR spectrum of *B. mori* silk fibroin in aqueous solution (8.7 w/v %). The number of accumulations was ~40 000 and the time interval between pulses was 3 s. The carbonyl resonance region was expanded and inserted in the Figure.

C=O coincided with the singlet peak positions of *B. mori*. The other components of the Ala resonance in the *P. c. ricini* spectrum were assigned to the α-helical portion in the chain since these peaks shifted to other positions when urea was added to the solution and since the presence of the α-helix in *P. c. ricini* silk fibroin has been confirmed by ORD measurements.[21] These results indicate that there is no α-helical portion in the liquid silk of *B. mori*.[2]

It has been suggested that there are roughly two domains in the silk fibroin from *B. mori*. This conclusion is based on the amino acid analysis of the insoluble and soluble fractions of the protein treated with α-chymotrypsin, as summarized in Table II.[22-24] The insoluble (C_p) fraction consists approximately of Gly, L-Ala, and L-Ser residues and is considered to be a crystalline domain in the protein. The soluble fraction is a noncrystalline part which contains relatively large amounts of other amino acids. It is important to examine whether or not ^{13}C NMR spectroscopy may observe both domains of the fibroin simultaneously. The amino acid composition determined from the ^{13}C NMR spectrum without NOE is very close to that of the silk fibroin without any treatment and differs markedly from that of the soluble fraction. Thus, it is concluded that both domains, i.e., crystalline and noncrystalline domains, are observed in the ^{13}C NMR spectrum.

Table II
Amino Acid Composition of *B. mori* Silk Fibroin (mol %)

	silk fibroin[a]	silk fibroin[b]	C_p fraction[c]	C_s fraction[d]
Gly	42.9	42.9	48.0	36.85
Ala	29.9	30.0	32.89	22.16
Ser	11.6	12.2	14.97	6.96
Tyr	4.2	4.8	1.40	10.8
Val	1.4	2.5	0.64	5.67
Asp		1.9	0.56	3.87
Glu		1.4	0.43	2.58
Thr	0.4	0.9	0.36	2.32
Ile		0.6	0.13	1.80
Leu		0.6	0	1.29
Phe	0.4	0.7	0.13	1.54
Pro		0.5	0	1.03
Met		0.1	0	0
Cys		0.03	0	0
Lys		0.4	0.2	0.07
His		0.2	0.06	0.5
Arg		0.5	0.18	1.29

[a] Determined from ^{13}C NMR (this work). The content of the Gly residue was assumed to be 42.9%. The estimated errors were less than ±5%. [b] Data taken from ref 22. [c] Data taken from ref 23. [d] Data taken from ref 24.

Spin-Lattice Relaxation Times. Figure 2 shows a series of partially relaxed ^{13}C NMR spectra of the middle silk gland portion of intact mature larva of *B. mori*. Detailed peak assignments have been reported elsewhere.[2,15]

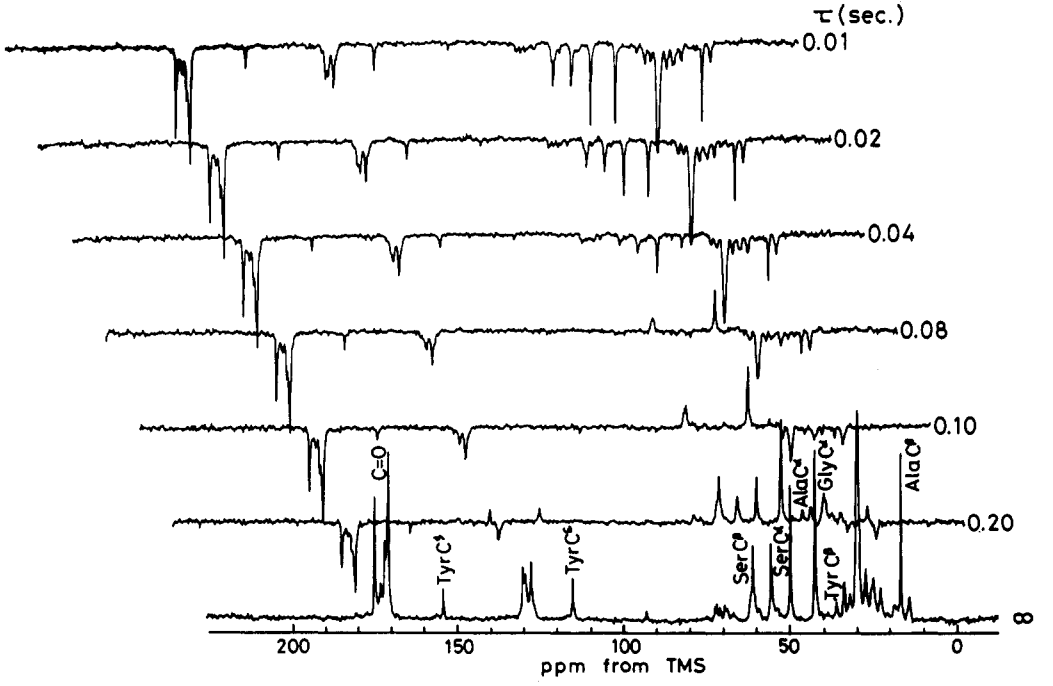

Figure 2. Partially relaxed ^{13}C NMR spectra of the silk gland portion of intact *B. mori* mature larva. The number of accumulations was 4000 for each spectrum. The ^{1}H nuclei were decoupled only during the sampling time of 0.34 s. τ was the delay time between the 180° and 90° pulses and the waiting time was 4 s.

Table III
Spin-Lattice Relaxation Times (T_1's) as a Function of the Concentrations and Nuclear Overhauser Enhancements (NOE's) of *B. mori* Silk Fibroin in Aqueous Solution

amino acid	T_1, s											
	2.1[a]	2.7	4.2	5.6	5.9	7.5	8.1[b]	8.8	9.6	14.5	30[c]	NOE[d]
Ala												
C^α	0.28	0.31	0.28	0.26	0.28	0.26	0.24	0.26	0.23	0.25	0.19	2.2
C^β	0.35	0.45	0.45	0.43	0.37	0.41	0.35	0.42	0.45	0.41	0.37	2.5
Gly												
C^α	0.15	0.15	0.15	0.15	0.12	0.13	0.12	0.15	0.12	0.12	0.11	2.2
Ser												
C^α	0.26	0.26	0.23	0.23	0.21	0.21	0.22	0.21	0.25	0.22	0.20	2.3
C^β	0.20	0.19	0.18	0.17	0.15	0.16	0.12	0.15	0.17	0.15	0.11	2.3
Tyr												
C^β	0.19	0.15	0.13	0.09	0.12	0.12		0.11		0.10	0.07	
C^δ	0.27	0.22	0.23	0.22	0.20	0.21		0.19	0.23	0.19		2.0
C^ϵ	0.28	0.22	0.24	0.20	0.21	0.19		0.20	0.22	0.21	0.18	2.3

[a] Concentration in w/v %. [b] The silk fibroin solution prepared from the liquid silk stored in the silk gland of *B. mori*. [c] In *B. mori* mature larva. [d] Averaged over the concentrations.

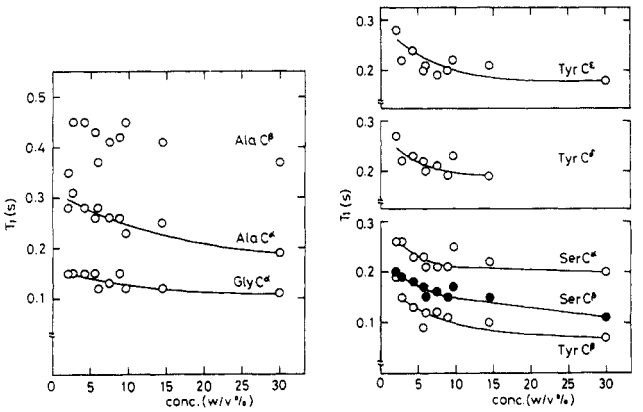

Figure 3. Concentration dependence of the spin-lattice relaxation times (T_1) of *B. mori* silk fibroin.

In the middle silk gland, there are two kinds of silk protein, i.e., silk fibroin and sericin, although the former is dominant.[5] However, the plots of $M_0 - M_z$ vs. τ for the carbons of the Ala, Gly, Ser, and Tyr residues are essentially single exponential, where M_0 is the equilibrium amplitude of the fully relaxed spectrum, M_z is the amplitude of a partially relaxed spectrum, and τ is the delay time between the 180° and 90° pulses. Thus, it is likely that the T_1 values obtained here reflect those of silk fibroin. The T_1 determinations were performed as a function of concentration from 2.1% to 14.5% for the regenerated silk fibroin. The T_1 values are summarized in Table III and plotted against concentration in Figure 3. As described in the Experimental Section, the regenerated fibroin solution of arbitrary concentration is prepared by a relatively complex process since the degummed silk is insoluble in water directly. This might lead to some scattering in the plot of T_1 vs. concentration. But it is likely that T_1 values decrease gradually with increasing concentration except for the Ala C^β, where the data show a large scattering. All T_1 values of liquid silk in intact silkworms are smaller, by 0.02–0.06 s, than the corresponding values for 14.5% regenerated silk fibroin. Since the concentration of the liquid silk in the middle silk gland of *B. mori* mature larvae is reported as ca. 30%,[25] this T_1 value will also be dependent on the concentration. Moreover, the T_1 values were determined for the 8.1% solution of the silk fibroin obtained directly from the silk protein stored in the silk gland after sericin was removed.[25] The data indicate a similar trend of the concentration-dependent T_1 behavior within experimental error. Appearance of the silk I type conformation[26] accompanying the aggregation of the fibroin chain is considered to be the origin, as discussed later.

We will examine the motion of the silk fibroin qualitatively here and a more quantitative description of the segmental motion will be given in the next section. The NT_1 values obtained for the α-carbons, where N is the number of directly attached hydrogen atoms to the given carbon, were approximately the same for the Ala, Gly, and Ser residues (0.26–0.30 s in the 2.1% solution and 0.19–0.22 s in the liquid silk), indicating isotropic segmental motion of the chain. As for the motion of the side group, the NT_1 values of the C^β carbons were 1.1–1.4 s for the Ala residue, 0.22–0.40 s for the Ser residue, and 0.14–0.38 s for the Tyr residue. Thus, the rate of internal rotation around the C^α–C^β bond decreases in the order Ala, Ser, Tyr. Especially, the comparable NT_1 value of the Tyr C^β carbon relative to those of the C^α carbons indicates that internal rotation of the C^α–C^β bond is strongly hindered.[27] Similarly, the NT_1 values of the aromatic carbons, C^δ and C^ϵ, of the Tyr residue are 0.18–0.28 s, indicating that the rotation around the β–γ axis is also strongly hindered. Although these data might suggest that there are an intra- and/or intermolecular hydrogen bond formation between any amino acid residues and the Tyr OH group, this possibility is excluded by the pK_a value for the deprotonation, as described below.

Mean Correlation Time for the Segmental Motion of *B. mori* Silk Fibroin. In order to determine the correlation time for the backbone segmental motion of the silk fibroin quantitatively, NOE as well as T_1 values were measured as a function of concentration. However, we could not judge from the data whether the NOE values were concentration dependent or not, because of the large scattering. Therefore, the NOE values were averaged over all the concentrations for each carbon (Table III).

The NT_1 and NOE values averaged over the Ala, Gly, and Ser C^α carbons are used to determine the correlation times of the segmental motion. The NOE value of 2.2 deviates appreciably from the theoretical maximum value 2.988, which indicates that the extreme narrowing condition is no longer applicable in describing the chain motion.[7] Moreover, a correlation time which satisfied both the T_1 and NOE data was not obtained when a general isotropic rotational diffusion model[7] (single correlation time model) was used. Therefore, the log χ^2 distribution model was applied to determine the correlation time for the segmental motion of silk fibroin as a function of the concentration. The interpretation of the model is given in detail elsewhere.[8] The results are shown in Figure 4.

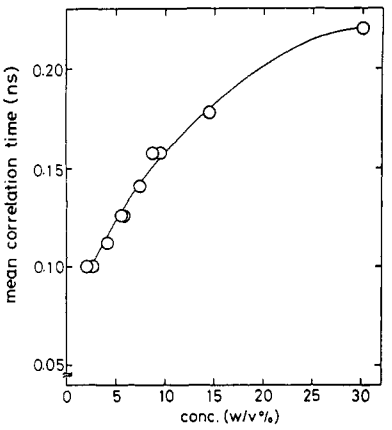

Figure 4. Concentration dependence of the mean correlation times for the segmental motion of *B. mori* silk fibroin determined from NT_1 and NOE values averaged over Gly C^α, Ala C^α, and Ser C^α assuming the log χ^2 distribution model. The width parameters in the model were 10–14. The NOE value for the liquid silk in the *B. mori* silk gland was assumed as 2.2.

With increasing concentration, the mean correlation time increases gradually from 0.10 ns (2%) to 0.22 ns (30%). These are within the values typical of a random coil polymer, 0.1–1.0 ns at 30–40 °C.[7] Moreover, the width parameter, p, in the log χ^2 distribution model was relatively small, 10–14, indicating a broad distribution of the correlation time. This is also typical of a random coil polymer.[7]

pH Dependence. The relaxation behavior of the Tyr residue of the silk fibroin shows a somewhat restricted side-chain motion. In order to examine whether hydrogen bonds are formed between any amino acid residues and the OH group, spectra of the silk fibroin were observed as a function of pH. Since gelation of *B. mori* silk fibroin solution takes place in the acidic pH range, the NMR observations were performed in the neutral and alkaline pH range. In these pH ranges, a chemical shift change due to the deprotonation of Tyr side group occurs, as shown in Figure 5. Using the Henderson–Hasselbalch equation,[28] we determined the pK_a value by curve fitting to be 10.1 in the 8% solution. This is an average value for the Tyr C^γ, C^ϵ, C^ζ, and C=O carbons. Similar pH titration experiments were performed for the 2.2% and 5.3% solutions and the resulting pK_a values were 10.3 and 9.8, respectively. Thus, the pK_a value is independent of the concentration, within the limits of experimental error. Figure 6 shows the pH titration curve of the NMR chemical shifts of the Ac-X-NHMe mixture where the amino acid composition

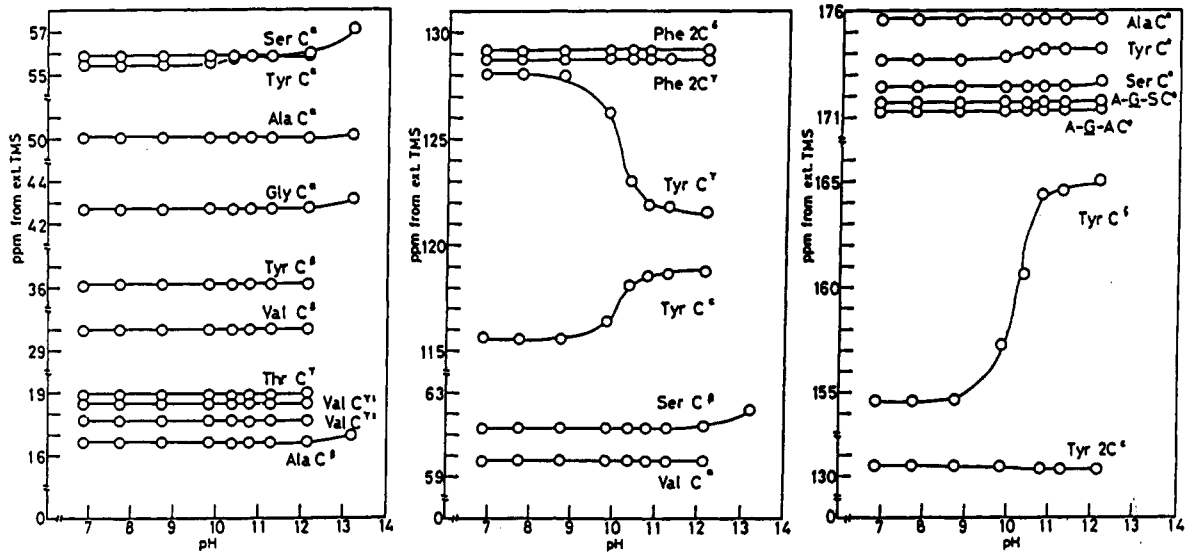

Figure 5. pH dependence of the ^{13}C NMR chemical shifts of *B. mori* silk fibroin (8.2 w/v %).

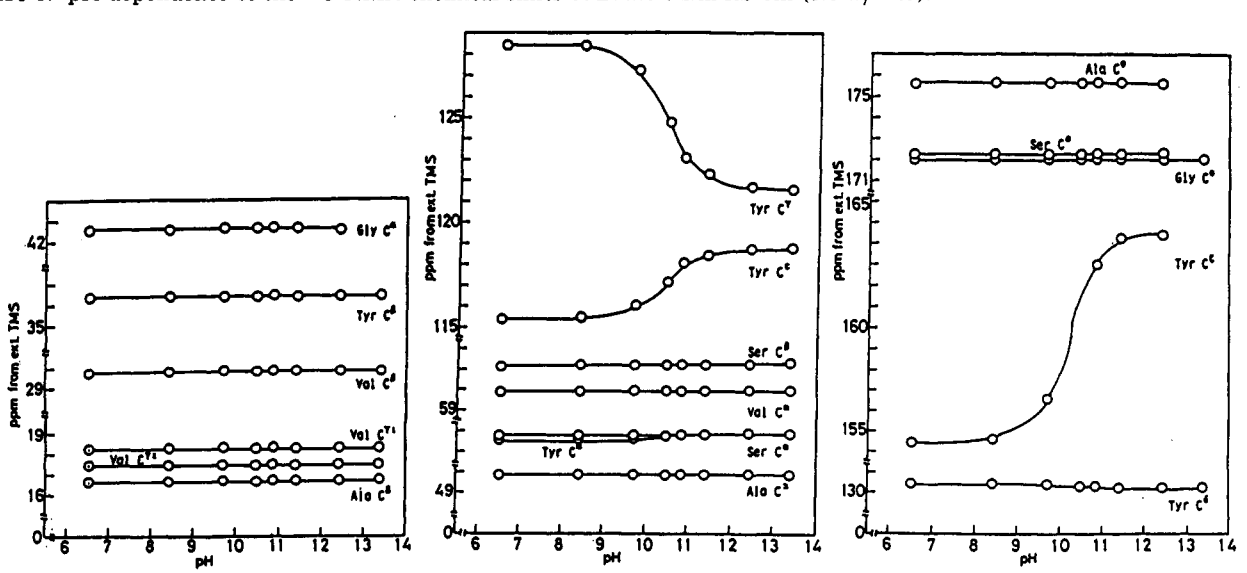

Figure 6. pH dependence of the ^{13}C NMR chemical shifts of the mixture of Ac-X-NHMe, where X = Gly, L-Ala, L-Ser, L-Tyr, and L-Val (5 w/v %). The composition of the mixture was the same as that of *B. mori* silk fibroin.

is the same as in silk fibroin in the same pH range. The pK_a value resulting from the Tyr OH deprotonation of Ac-Tyr-NHMe was also 10.3. This value agrees with the pK_a value obtained for silk fibroin, indicating a similar degree of solvent/Tyr hydrogen bonding and a lack of hydrogen bonding between the Tyr OH group and the amino acid residues of the silk fibroin.

Moreover, marked downfield shifts of the Ser C^α and C^β peaks were observed in the pH titration curve of the silk fibroin at the pH range from 11 to 13.5 although there were no changes in the chemical shift of Ac-Ser-NHMe at the same pH range. This change in chemical shift has been also observed for the Ser C^α and C^β carbons of luteinizing hormone-releasing hormone between pH 10.5 and 12.7.[29]

Discussion

The chain dynamics of *B. mori* silk fibroin may be characterized by both the very small value of the order of 10^{-10} s and a broad distribution of the correlation times for the segmental motion at 40 °C. This is a typical trend of the motional behavior of a random coil polymer in solution. The structure of *B. mori* silk fibroin in aqueous solution or in the middle silk gland has been studied by many investigators.[25] The solution structure depends on concentration. A random coil conformation has been proposed in dilute aqueous solution. However, there are some uncertainties about the conformation in concentrated solution or when the protein is stored in the middle silk gland of the silkworm. An intramolecular β-type has been proposed by Iizuka et al.[30,31] using the methods of light scattering, intrinsic viscosity, flow birefringence, CD, ORD, and IR. However, a more recent study using the laser Raman spectrum method, indicates that both random coil (1260 and 1660 cm^{-1}) and α-helix (947 cm^{-1}) portions occur in the chain.[32] A direct ^{13}C NMR spectroscopic comparison of the silk fibroin stored in the silk glands of intact *B. mori* and *P. c. ricini* mature larvae rules out the presence of α-helical portions in the *B. mori* silk fibroin.[2] Also, Kobayashi et al.[33] concluded from the CD pattern, which has two broad troughs at 218 and 206 nm, that the helical conformation occurs in aqueous solutions of *B. mori* fibroin at concentrations higher than 5%. The helix content was described from the ORD measurement as a function of the concentration. The conformation is a random coil at less than ca. 5% concentration, but the helix content increases dramatically with increasing concentration and reaches 40% in the 20% solution. The authors concluded that the helix detected in the *B. mori* silk fibroin solution is the silk I type (loose helix)[26] rather than the α-helical type since the positions of the troughs in the CD spectrum differ slightly from the corresponding position which characterize an α-helix (222 and 206 nm).[30] Thus, it is interesting to examine the concentration dependence of the molecular motion of the silk fibroin. The T_1 data and also the correlation times for the segmental motion decrease gradually with increasing concentration as shown in Figures 3 and 4. This appears to correlate with the CD and ORD data by Kobayashi et al., who suggest the appearance of the silk I type conformation in concentrated solution. However, aggregation of *B. mori* silk fibroin in concentrated aqueous solution has been also reported by Kratky[34] by small-angle X-ray scattering. The silk fibroin appeared as a rodlike particle with a 60 × 90 Å cross section over a 10–20% concentration range. The decreased cross section was observed at 8.8% and the scattering was no longer observed for a 4.1% solution. The aggregation of the chain may also cause the decrease in the chain motion of the silk fibroin and thus, we could not separate the effect of the aggregation on the molecular dynamics from the conformational change. A further study is now proceeding in our laboratory i.e., measurements of $^3J_{C'-N-C^\alpha-H}$ coupling constant in the spectra of [1-^{13}C-Gly] and [1-^{13}C-Ala] silk fibroins from *B. mori* as a function of concentration, because the coupling constant gives a direct information on internal rotation angle around the N–C^α bond of amino acid residues. In addition, a detailed study on the structure of Silk I type silk fibroin in solid state is proceeding by us using solid-state high-resolution ^{13}C NMR (CP/MAS NMR). Since the ^{13}C chemical shift is independent of the concentration, the electronic state of all the ^{13}C nuclei of *B. mori* silk fibroin is not influenced by the interactions which cause the change in the T_1 values.

References and Notes

(1) Torchia, D. A.; VanderHart, D. L. "Topics in Carbon-13 NMR Spectroscopy"; Levy, G. C., Ed.; Wiley-Interscience New York, 1976; Vol. 3, p 325.
(2) Asakura, T.; Watanabe, Y.; Suzuki, H. *Macromolecules* **1983**, *16*, 1024.
(3) Saito, H.; Iwanaga, Y.; Tabeta, R.; Narita, M.; Asakura, T. *Chem. Lett.* **1983**, 427.
(4) Kricheldorf, H. R.; Müller, D.; Ziegler, K. *Poly. Bull.* **1983**, *9*, 284.
(5) Fraser, R. D. B.; MacRae, T. P. "Conformation in Fibrous Proteins"; Academic Press: New York and London, 1973.
(6) Farrar, T. C.; Becker, E. D. "Pulse and Fourier Transform NMR"; Academic Press: New York, 1971.
(7) Heatley, F. *Prog. NMR Spectrosc.* **1979**, *13*, 47.
(8) Schaefer, J. *Macromolecules* **1973**, *6*, 882.
(9) Lyerla, J. R., Jr.; Horikawa, T. T.; Johnson, D. E. *J. Am. Chem. Soc.* **1977**, *99*, 2463.
(10) Heatley, F.; Begum, A. *Polymer* **1976**, *17*, 399.
(11) Asakura, T.; Suzuki, K.; Horie, K.; Mita, S. *Makromol. Chem.* **1981**, *182*, 2289.
(12) Asakura, T.; Doi, Y. *Macromolecules* **1983**, *16*, 786.
(13) Saito, H.; Ohki, T.; Kodama, M.; Nagata, C. *Biopolymers* **1978**, *17*, 2587.
(14) For example: Ugurbil, K.; Norton, R. S.; Allerhand, A.; Bersohn, R. *Biochemistry 1977, 16*, 886.
(15) Asakura, T.; Ando, M. *Makromol. Chem., Rapid Commun.* **1982**, *3*, 723.
(16) Asakura, T.; Kamio, M.; Nishioka, A. *Biopolymers* **1979**, *18*, 467.
(17) Applewhite, T. H.; Niemann, C. *J. Am. Chem. Soc.* **1959**, *81*, 2208.
(18) Opella, S. J.; Nelson, D. J.; Jardetzky, O. *J. Chem. Phys.* **1976**, *64*, 2533.
(19) Howarth, O. W.; Lilley, D. M. *Prog. NMR Spectrosc.* **1978**, *12*, 1.
(20) In some spectra of intact *P. c. ricini* and *A. pernyi* silkworms, the Ala C^α carbon was observed as a triplet peak, 50.1, 50.8, and 51.5 ppm. The central peak of 50.8 ppm was assigned to the C^α carbon of the alanine monomer in the silk gland from the chemical shift and disappeared when only liquid silk obtained from *P. c. ricini* mature larva was observed.
(21) Iizuka, E. *Biochim. Biophys. Acta* **1968**, *160*, 454.
(22) Shimura, K. "Zoku Kenshi no Kozo"; Hojo, N., Ed.; Shinshu University: Ueda, 1976; p 337.
(23) Strydom, D. J.; Haylett, T.; Stead, R. H. *Biochem. Biophys. Res. Commun.* **1977**, *3*, 932.
(24) Lucas, F.; Shaw, J. T. B.; Smith, S. G. *Biochem. J.* **1957**, *66*, 468.
(25) Komatsu, K. *Hikaku Kagaku* **1982**, 27, 193.
(26) Silk I, a crystalline modification, was obtained when the silk gland content was dried gently without mechanical disturbance and when the silk or the C_p fraction was dissolved in aqueous LiBr. Since this modification is less stable than the silk II type (antiparallel β sheet), another crystalline modification, the structure is far less definitely established. Konishi et al. reported the unit cell demension for the C_p fraction crystalline from dilute LiBr/water solution as a = 4.59, b = 9.08 (fiber repeat distance), and c = 7.20 Å. The translation along the molecular axis calculated from the b value was 2.27 Å, which is longer than the corresponding value for the α-helix (1.5 Å) and shorter than the silk II type (3.5 Å). This indicates that the silk I type conformation is a loose helix. Konishi, T.; Kurokawa, M. *Sen-i Gakkaishi* **1968**, *24*, 550.
(27) On the basis of the measured NT_1 values, we compared the rate of internal motion about the C^α–C^β bond among the Ala, Ser, and Tyr residues qualitatively. However, since the NT_1 values are sensitive to both the rate and amplitude of the

side-chain reorientation, it seems necessary to discuss these two factors separately in a more quantitative approach concerning the side-chain motion. Lipari, G.; Szabo, A. *J. Am. Chem. Soc.* **1982**, *104*, 4546.
(28) Wüthrich, K. "NMR in Biological Reseach. Peptide and Proteins"; North-Holland Publishing Co.: Amsterdam, 1976.
(29) Smith, I. C. P.; Deslauriers, R.; Saito, H.; Walter, R.; Garrigou-Lagrange, C.; McGregor, H.; Sarantakis, D. *Ann. N.Y. Acad. Sci.* **1973**, *222*, 597.
(30) Iizuka, E.; Yang, J. T. *Proc. Natl. Acad. Sci. U.S.A.* **1966**, *55*, 1175.
(31) Iizuka, E.; Yang, J. T. *Biochemistry* **1968**, *7*, 2218.
(32) Magoshi, J.; Magoshi, Y.; Kamiyama, S.; Nakamura, S. *Polym. Prepr., Jpn.* **1981**, *30*, 1616.
(33) Kobayashi, Y.; Fujiwara, T.; Kyogoku, Y.; Kataoka, K. "Abstracts of the 19th Meeting of Nuclear Magnetic Resonance in Japan", 1980, p 149.
(34) Kratky, O. *Z. naturforsch B*, **1955**, *10B*, 510.

Solid-State ^{13}C NMR Study of Resol-Type Phenol–Formaldehyde Resins

Gary E. Maciel* and I-Ssuer Chuang

Department of Chemistry, Colorado State University, Fort Collins, Colorado 80523

Lawrence Gollob†

Department of Forest Products, Oregon State University, Corvallis, Oregon 97331.
Received February 23, 1983

ABSTRACT: The ^{13}C NMR experiment with cross polarization (CP) and magic-angle spinning (MAS) provides valuable information on the structure and the curing process of the resol-type phenol–formaldehyde resins. Two major features revealed by this technique regarding the curing process of these resins are the extensive involvements of the hydroxyl group of phenols and condensation of methylene bridges with hydroxyl groups.

Introduction

The technical development of the first fully synthetic resins, the phenol–formaldehyde resins formed from the reaction of phenol with formaldehyde, proceeded very rapidly after the discoveries of Baekeland.[1,2] However, the scientific investigation of the basic chemistry of these resins lagged far behind. The structural pecularities of these resins are due to the polyfunctionality of phenol, i.e., more than one site for aromatic substitution reactions. Under different sets of conditions (e.g., temperature, pH value, catalyst,...), the resins will show differences in their isomeric compositions, chain length, etc. The specific details of the structure of a phenol–formaldehyde resin have a substantial effect on the nature, extent, and rate of hardening.[1-3] Therefore, it is tremendously important to understand the reaction details of different stages in the formation of the phenol–formaldehyde resins under different sets of reaction conditions and their effects on the structures of these resins.

During the 1940s and 1950s there was considerable effort put on the study of reactions between phenols and formaldehyde.[4-10] Due to the very large varieties of compounds occurring in the reaction mixtures, researchers simplified the situation by employing some positionally blocked compounds as model substances to study the kinetics of reaction. Although these partially blocked compounds cannot truly reflect the actual situation occurring in phenol–formaldehyde in the reaction mixtures, these studies did provide valuable information concerning the reaction between phenol and formaldehyde under different sets of conditions. On the basis of these earlier studies, later IR,[6a,11-13] ^1H NMR,[14,18c] and ^{13}C NMR[15-21] studies have provided many more details of the reactions between phenols and formaldehyde. During the past several years ^{13}C NMR studies have yielded useful information concerning the positions of linkage between the phenol rings. However, nearly all the ^{13}C NMR studies reported so far[21] have been carried out on the liquid solution state, which has the disadvantage of possible influence of solvent and severe solubility problems for cured resins. Recent papers have dealt with the ^{13}C NMR study of solid phenolic resins.[21]

In recent years there have been major advances in solid-state high-resolution ^{13}C NMR. By combination of cross polarization[22] with high-power ^1H decoupling, accompanied by high-speed magic-angle spinning techniques[23] (CP/MAS), one can obtain high-resolution ^{13}C NMR spectra of solid materials. Excellent review articles[24] have recently appeared concerning the applications of this powerful technique in the study of polymers. These techniques are especially promising in the study of phenol–formaldehyde resins, because they provide the opportunity to study the insoluble resins under nondestructive conditions.

Experimental Section

The resin-forming reactions between phenol and formaldehyde were conducted at different molar ratios of formaldehyde to phenol and different initial catalyst (sodium hydroxide) levels. A summary of these conditions and some properties of the resulting resins are given in Table I. Four samples derived from each resin were studied, each representing a different state or extent of polymerization. Each of the four sample types is identified by a suffix after the sample number as follows: a very viscous, tarlike resin (l); a freeze-dried resin from dioxane/water after neutralization with acetic acid (n); a freeze-dried resin from water, nonneutralized (non); a resin cured at 110 °C for more than 24 h (cured). The curing experiments were carried out with thin films of resin on sheets of glass at 110 °C. This is not necessarily a good mimic of curing in a glue line.

The ^{13}C NMR spectra were recorded on a JEOL FX-60QS spectrometer by the CP/MAS technique. The spectra were taken under various contact times (0.03–10 ms) with a 1-s repetition time. Each sample was examined with a MAS spinning rate around 2.2 kHz. The magic-angle setting was checked before and after each ^{13}C CP/MAS experiment by the ^{79}Br–KBr method.[32] In some experiments a pulse sequence described by Opella and co-workers[25] was used in which a delay is inserted (during which there is no decoupling) between the CP contact period and data acquisition; during this interrupt period those carbons having directly attached protons (except those of rapidly rotating methyl groups) are distinguished from those carbons having no directly attached proton(s), because of the grossly different intensities

† Present address: Georgia Pacific Corporation, Decatur, GA 30035.

0024-9297/84/2217-1081$01.50/0